Chain End Effects and Dewetting in Thin Polymer Films

G. Henn,[†] D. G. Bucknall,[‡] M. Stamm,*[,†] P. Vanhoorne,[§] and R. Jérôme[§]

Max-Planck Institut für Polymerforschung, Ackermannweg 10, Postfach 3148, D-55021 Mainz, Germany, ISIS Facility, Rutherford Appleton Laboratory, Didcot, U.K., and Center for Education and Research on Macromolecules, University of Liège, Sart-Tilman B6, B-4000 Liège, Belgium

Received January 20, 1995; Revised Manuscript Received January 9, 1996[⊗]

ABSTRACT: The dewetting of thin films of end-functionalized polymers, ω- and α,ω-barium sulfonato polystyrenes, on a silicon substrate has been investigated as a function of initial film thickness, molecular weight, and functionality of the chains. The lower molecular weight monofunctional chains are found to dewet the substrate analogously to normal polystyrene but display an anomalous flow behavior at the surface. Moreover, after dewetting, the entire silicon surface still remains covered by a monolayer of monofunctional chains. The monolayer consists of a polymer brush of densely packed tethered chains, adsorbed via their ionic end groups. The dense packing and special conformations of the chains in the brush prevent interpenetration with other polymer chains, and the unadsorbed macromolecules dewet the brush. When the molecular weight of the monofunctional chains is increased, entanglements between the adsorbed polymer brush and the unadsorbed chains can occur and the dewetting process is retarded. Thin films of the difunctional chains do not dewet regardless of the molecular weight of the chains. The difference between mono- and difunctional materials is attributed to ionic aggregation, which is responsible for thermoreversible cross-linking and stabilization of thicker films by interaction of aggregates with dangling ends. It is suggested to use high molecular weight end-functionalized chains as polymeric additives to retard thin polymer film dewetting.

Introduction

Thin polymer films are increasingly used in technological applications like coatings, dielectrics, biomedical devices, nonlinear optics, and numerous other fields. In these cases, the films are required to remain homogeneous, stable, and of uniform thickness. Under some circumstances, such as electronic applications, these film properties are essential even under stringent environmental and thermal treatment. Using techniques like spin-coating, polymer films can be prepared even on nonwettable surfaces. However, while thick polymer films (whose thickness is greater than a few micrometers) may be stable or metastable due to gravity,[1,2] thinner films are intrinsically unstable due to intermolecular forces.[3] When heated above the glass transition temperature, these films break up and spontaneously dewet the substrate, resulting in the formation of droplets.[4,5] The dewetting process has recently been studied, both theoretically[6−8] and experimentally.[9−12]

The stabilization of thin polymer films is therefore of the utmost importance for many industrial applications. Usual methods for stabilizing nonwetting films rely upon the modification of the interfacial tension between the liquid and the substrate. Widespread methods used to change the wettability of a substrate are chemical surface modifications, *e.g.*, plasma treatment or reaction with surface-active agents. An alternative approach proposed here is the use of end-functionalized polymer chains, which are able to form a polymer "brush" adsorbed on the substrate via the "sticky" end groups.[13] Entanglements between the tethered and free polymer chains in the thin film can prevent dewetting from occurring, as has been recently evidenced by Yerushalmi *et al.*[14] A wide range of functional groups may promote the tethering of the chains,[13] among which ionic groups have been shown to be highly efficient.[15,16] In this paper the effect of end sulfonation on the thermal stability of thin polystyrene films deposited onto silicon substrates is investigated. In particular the influence of the molecular parameters, such as molecular weight and functionality of the chains, on the dewetting process is demonstrated, and the formation of a stabile monolayer below the dewetting film is shown to exist in some cases revealing the astonishing fact that polymer chains may show dewetting on top of a film of identical chemical composition.

Experimental Section

Polymer Synthesis. ω- And α,ω-sulfonato polystyrene samples were synthesized by living anionic polymerization of styrene followed by deactivation with 1,3-propane sultone, as reported elsewhere.[17] Functionality was systematically better than 90%, as checked by potentiometric titration of the acid end groups with a standard solution of tetramethylammonium hydroxide in a toluene/methanol (9/1, v/v) mixture. Molecular weight and molecular weight distribution were measured by size exclusion chromatography of a polymer sample picked out before deactivation of the living chains by 1,3-propane sultone.

Lithium sulfonate-terminated polymers were converted into the barium form via the formation of the acid form produced by repeated precipitation in methanol containing at least 20 equiv of perchloric acid and a final reprecipitation in pure methanol. (Semi)telechelics were kept in the acid form in a toluene/methanol solution. Sulfonic acid end groups were neutralized by 1.05 equiv of barium acetate. Methanol and acetic acid were removed by the azeotropic distillation of the solvent (regularly replaced by dry toluene), until no polar compound could be detected in the distillate by gas chromatography and/or potentiometric titration. The solvent was finally removed by distillation. All the samples were dried at 160 °C, under vacuum, for 16 h.

Dewetting Experiments. Thin polymer films were spun cast from dilute toluene solutions onto clean silicon wafers kindly supplied by Wacker Chemitronics, Burghausen, Germany. Film thicknesses were measured using X-ray reflectivity utilizing a setup at an 18 kW rotating anode generator

* To whom correspondence should be addressed.
[†] Max-Planck Institut für Polymerforschung.
[‡] Rutherford Appleton Laboratory.
[§] University of Liège.
[⊗] Abstract published in *Advance ACS Abstracts,* May 1, 1996.

S0024-9297(95)00039-8 CCC: $12.00

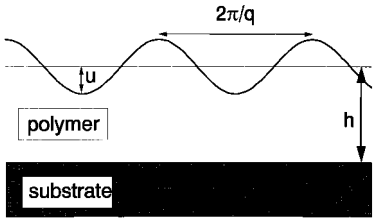

Figure 1. Schematic illustration of the surface modulations of an initially uniform film of thickness h. The oscillatory amplitude is u, and the lateral oscillation wavevector is q.

at a wavelength of 0.154 nm.[18,19] Most films were annealed in a vacuum oven, and only a few samples were heated for a few minutes directly in the hot stage of the optical microscope. No differences between samples annealed either in air or under vacuum could be detected. Annealing temperatures and times varied from 160 to 175 °C and from 10 min to 200 h, respectively. The occurrence of the dewetting process does not depend on the temperature at which the samples were annealed, but at lower temperatures the dynamics are slower mainly due to a lower polymer diffusivity.

Dewetting dynamics were observed using an optical microscope in reflection mode (Zeiss, Germany) fitted with a CCD video camera and a heating stage. The surface heterogeneities were obtained using an optical phase interference measurement microscope (Maxim 3D, Zygo Corp.). X-ray reflectivity was used to follow film thickness changes during dewetting and to measure the final film thickness after the annealing process.

Theory

In a liquid film, thermal fluctuations cause thickness modulations which may be expressed by eq 1:[6]

$$z(x,t) = h + u \exp(iqx) \exp(-t/\tau_r) \tag{1}$$

where x is a coordinate parallel to the surface, h the initial uniform film thickness, u the oscillatory amplitude of the surface modulations, q the wavevector, t the time, and τ_r the relaxation time (see Figure 1).

However, intermolecular forces, such as van der Waals forces, produce a disjoining pressure defined as:[6]

$$\Pi = -A/6\pi z^3 \tag{2}$$

where $A = A_{sl} - A_{ll}$ is the difference between the Hamaker constants for solid−liquid interactions (A_{sl}) and liquid−liquid interactions (A_{ll}). The sign of A indicates whether the molecules of the liquid are more attracted by the substrate or by like molecules. Π thus expresses the tendency of the film to adjust its thickness in order to minimize the free energy.

The surface tension γ, by contrast, tries to reduce the surface fluctuations, a tendency which is expressed by the Laplace pressure:[6]

$$P_L = \gamma(d^2z/dx^2) \tag{3}$$

The balance between these two pressures determines whether the surface modulations are damped or amplified, which may lead in the latter case to the formation of holes and finally to the dewetting of the film. If A is positive, the oscillations are damped and the film is stable. For negative values of A, the film tends to get thinner and the surface oscillations are amplified. From

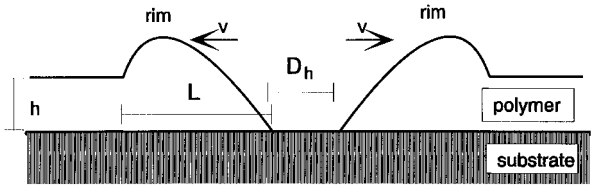

Figure 2. Schematic illustration of a cross section through a hole at early stages of dewetting. The material from the center part of the hole is collected in the rim at the edges of the hole. h is the initial film thickness, D_h the hole diameter, L the width of the rim, and v the velocity of the dewetting liquid.

mass conservation considerations, it has been shown[6] that, for $A < 0$, the fluctuations of the film surface are amplified exponentially with some resemblence to spinodal decomposition with a fastest growing wavevector:

$$q_m = \left(\frac{3}{2}\right)^{1/2} \frac{(|A|/6\pi\gamma)^{1/2}}{h^2} \tag{4}$$

From eq 4, it can be seen that the thickness fluctuations responsible for the hole formation have a wavelength proportional to h^2. Therefore, the average distance between holes during dewetting is also expected to be proportional to h^2 and thus depends strongly on the initial thickness of the film.

The amplification of the surface modulations creates an initially random pattern of holes that grow, pushing a rim of liquid ahead (Figure 2). When two rims meet, they form a liquid ribbon that breaks into droplets due to Rayleigh instabilities.[5] The diameter of the droplets, D_d, is proportional to the width of the rim and depends on the initial film thickness, h, and the contact angle between liquid and substrate, θ_E.[7,9]

At the final stage of the dewetting process, the droplets are arranged on a Voronoi cell pattern of polygons whose diameter is determined by the initial film thickness.[9] Since both the diameter of the droplets and the diameter of the polygons depend on the initial film thickness, h, the number of droplets per reference area, N_d, is also strongly dependent on h.[9]

The dynamics of hole formation in a polymer melt is different to the flow of a normal liquid. The difference occurs due to polymer slippage.[7,10] The slippage is characterized by the extrapolation length b, defined as the distance from the wall at which the velocity extrapolates to zero. Provided that the chains are not tethered to the wall by specific interactions, the extrapolation length of entangled polymers is given by:[7]

$$b = a(N^3/N_e^2) \tag{8}$$

where a is the size of the monomer unit, N is the degree of polymerization, and N_e is the critical degree of polymerization for entanglements. In the limit where $h > b$, the liquid flow at the surface obeys a Poiseuille type law.[7,10] The balance between the capillary forces and the viscous forces then results in a constant flow velocity, and the radius of the holes, R_h, grows linearly with time,[10] as expressed by eq 9:

$$R_h \propto t \tag{9}$$

On the other hand, when $h < b$, the Poiseuille flow is plugged. The melt slips at the surface and moves like

Table 1. Molecular Parameters of the Investigated End-Sulfonated Polystyrenes

$\bar{M}_n$	$\bar{M}_w$	$\bar{M}_w/\bar{M}_n$	F^a
2800	3000	1.07	0.92
13 000	14 000	1.08	0.96
18 000	19 500	1.08	0.92
19 500	20 500	1.05	0.94
82 000	98 000	1.20	0.90
98 000	100 000	1.02	0.93
7200	8500	1.18	1.86
14 000	17 000	1.21	1.90
102 000	109 000	1.07	1.88

[a] Average number of ionic end groups per chain.

a solid. As a result, the flow velocity decreases with time, and the hole radius growth is given by:[10]

$$R_h \propto t^{2/3} \tag{10}$$

As dewetting proceeds, for a film with $h < b$ the material from the dry patch collects in the rim, which thickens with time. At some point, when the actual thickness of the rim has grown to $h > b$, Poiseuille flow is restored and the flow velocity becomes constant.[10]

Results and Discussion

The molecular parameters of the investigated ω- and α,ω-barium sulfonate polystyrenes are summarized in Table 1. Molecular weight distributions are typical for anionic synthesis, and functionality F is systematically better than 0.9 for monofunctional samples and 1.85 for difunctional samples.

Low Molecular Weight ω-Barium Sulfonato Polystyrenes. Typical optical interference micrographs from a film of low molecular weight ($\bar{M}_n$ = 2800) ω-barium sulfonato polystyrene at different stages of dewetting are shown in Figure 3. After annealing the film (of thickness h = 24 nm) at a temperature of 175 °C for 20 min, holes form at random on the whole surface of the film and progressively grow with time, pushing a rim of liquid ahead. The optical interference patterns (Figure 3a−c) show a top view of the film, where the rims are seen as black rings around the holes. A topographic image is obtained after data processing of the interference patterns of Figure 3 (see Figure 4a), where a cross sectional view of a hole is displayed. When two rims come into contact, they form a ribbon which spontaneously decays into droplets (Figures 3b,c and 4b). At the final stage of dewetting (Figures 3d and 4c), a Voronoi pattern of polygons is formed, in which the edges are defined by the droplets of dewetted film. This behavior is entirely analogous to the dewetting as observed for nonfunctionalized polystyrene films on silicon substrates and reported by Reiter for different silicon wafer types.[9]

As expected from theory, the number of droplets, N_d, and the diameter of the droplets, D_d, strongly depend on the initial film thickness, h. The typical drop shape can be seen in Figure 4c and is clearly hemispherical. The scaling behavior of N_d and D_d with h is indicated in Figure 5. From the linear fits in the double-logarithmic plot of Figure 5, the power law dependencies of N_d and D_d with h have been fitted and are compared in Table 2 to the data of Reiter[9] for unfunctionalized polystyrene on two different silicon wafers. Clearly, no essential difference can be detected between unfunctionalized and ω-functional polystyrene chains.

Nevertheless, whereas the general dewetting behavior and final pattern of the dewetted film show no distinct differences with those of unfunctionalized polystyrene, anomalous dewetting dynamics is observed. Indeed, for thin polymer films (whose thickness is smaller than a few micrometers), the theory expects the radius of the

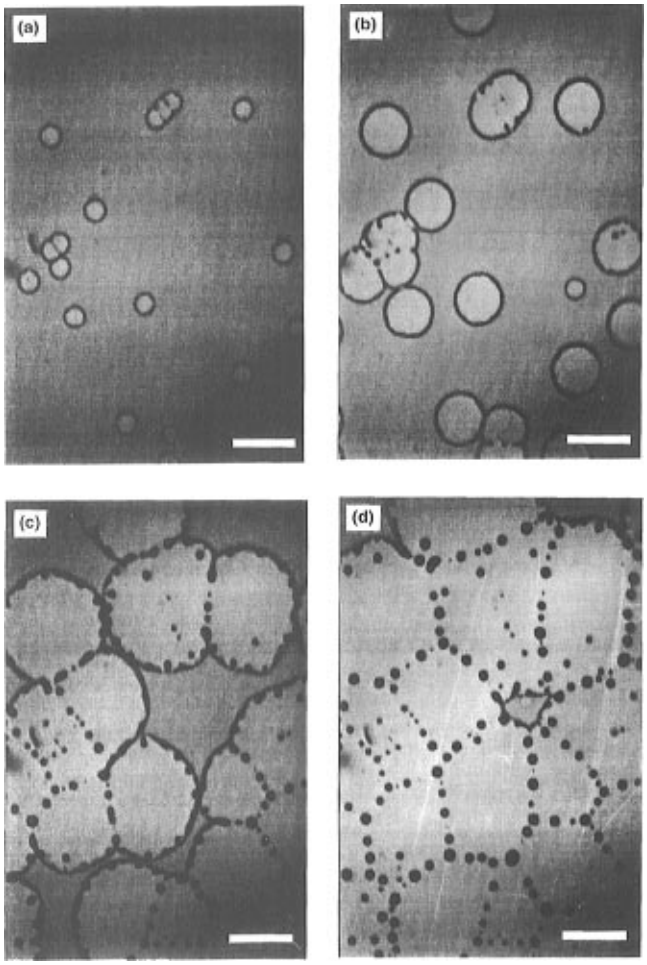

Figure 3. Optical interference micrographs of the time evolution of dewetting of ω-barium sulfonato polystyrene ($\bar{M}_n$ = 2800) with initial film thickness, h = 24 nm. Pictures are taken after (a) 20, (b) 50, (c) 120, and (d) 180 min total annealing time at 175 °C. The bar in each case represents 100 μm.

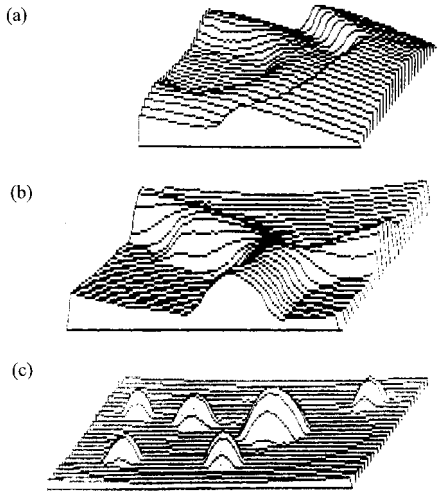

Figure 4. Optical phase measurement interference microscope pictures of different stages of dewetting of a ω-barium sulfonate polystyrene film: cross section through (a) a hole (42 × 42 μm^2, height scale 0−180 nm), (b) a ribbon (42 × 42 μm^2, height scale 0−180 nm), and (c) spherical droplets (78 × 58 μm^2, height scale 0−300 nm).

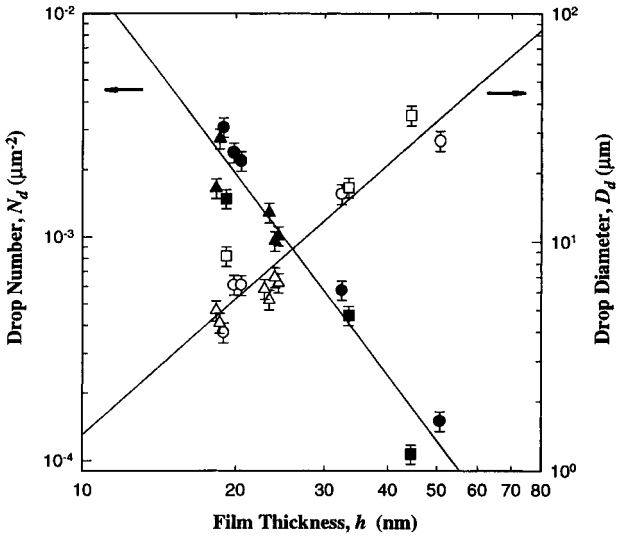

Figure 5. Double-logarithmic plot of drop number per reference area, N_d (filled symbols), and average drop diameter, D_d (open symbols), as a function of the initial film thickness, h. Average values were obtained from a minimum of five micrographs taken by optical phase interference (circles and squares) and classical optical microscopy (triangles). Molecular weight of the ω-barium sulfonato polystyrene was $\bar{M}_n = 2800$ (circles, triangles, and squares). The solid lines are best fits as explained in the text.

Table 2. Scaling Exponents of the Average Drop Number per Reference Area, N_d ($N_d \propto h^\alpha$), and the Average Drop Diameter, D_d ($D_d \propto h^\beta$), for Both Monofunctional $PS(SO_3)_2Ba$ ($\bar{M}_n = 2800$) and Unfunctionalized PS ($\bar{M}_n = 28\,000$)[a]

polymer	α	β
PS (SiA)[9]	−3.26 ± 0.14	1.54 ± 0.08
PS (SiB)[9]	−2.11 ± 0.09	1.05 ± 0.05
$PS(SO_3)_2Ba$	−3.1 ± 0.24	1.80 ± 0.20

[a] The data for normal polystyrene are reported by Reiter[9] and correspond to two different silicon surfaces labeled SiA and SiB.

holes to grow with the $^2/_3$ power of time, in agreement with eq 10. This time dependency can be seen as a consequence of polymer slippage at the surface of the substrate and has been experimentally observed by Redon *et al.*[10] for thin films of poly(dimethylsiloxane) deposited on silanized silicon wafers. The power law time dependency used to describe the experiments is given by eq 11:

$$R_h(t) = f(t + t_0)^x \qquad (11)$$

The initial time $t = 0$ is not exactly known and is thus replaced by the adjustable parameter t_0 in the fit; f, x, and t_0 are fit parameters.

Figure 6 shows the hole radius as a function of time for different film thicknesses. Obviously, the growth is not linear, and the polymer flow velocity is not constant. Fitting the hole growth curves by eq 11 gives the parameters reported in Table 3 for a series of films of varying thickness. t_0 can be put to zero for practical purposes. The average value of the exponent obtained from these fits is $x = 0.60$, which is very close to the theoretical value of $x = 0.67$ expected for the slippage of the polymer chains on the solid surface. Therefore, the dewetting process of low molecular weight ω-barium sulfonato polystyrenes can be characterized by a model assuming slippage of chains. In contrast, a different behavior has been observed by Reiter[9] for thin unfunctionalized polystyrene films on silicon wafers, where the

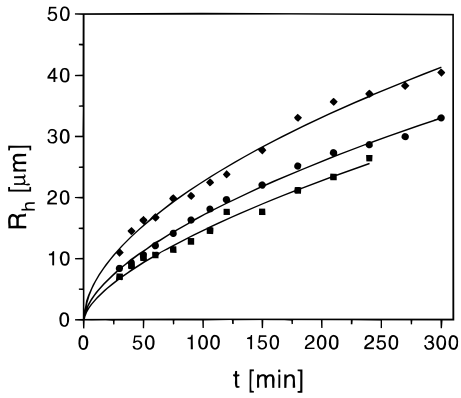

Figure 6. Hole radius, R_h, as a function of time for the dewetting of films of ω-barium sulfonato polystyrene ($\bar{M}_n$ = 13 000). Initial film thickness was h = 14 (■), 25 (●), and 33 (◆) nm. The solid lines are the best fits to eq 11 as described in the text.

Table 3. Experimental Parameters for the Power Law Equation Reported by Redon *et al.*[10] for the Time Evolution of the Hole Radius, R_h, during Dewetting of Thin Films of ω-Barium Sulfonato Polystyrene ($\bar{M}_n$ = 13 000)

h (nm)	a	t_0 (min)	x
14.0	0.76	2.0×10^{-7}	0.64
25.0	1.06	5.3×10^{-7}	0.60
33.0	1.79	1.2×10^{-8}	0.55

hole size has been found to scale linearly with time, as in the case of usual Poiseuille flow (eq 9). This apparent difference from our results might arise due to the higher flow velocity of unfunctionalized polystyrenes compared to the end-functionalized polystyrenes. In case of high flow velocities, it is hard to follow the exact power law of initial hole growth experimentally, and the corresponding time dependency may appear to be linear.

The dewetting process in addition has been followed by X-ray reflectometry. While optical microscopy can reveal the development of lateral structures, it gives only limited information on the film structure perpendicular to the film surface. This information is obtained from X-ray reflectometry, where, on the other hand, the pattern is averaged laterally and information about lateral structures is thus largely lost. The two techniques are thus complementary in an ideal way. Typical reflectivity curves are shown in Figures 7 and 8 before and after dewetting, respectively. For the unannealed films (Figure 7), the reflectivity curves show regularly spaced oscillations whose spacing is related to the thickness of the films (between 30 and 42 nm for the different samples). A typical surface roughness of the spin-cast films is obtained to be *ca.* 0.6 nm. After 200 h of annealing at 175 °C, the curves of Figure 8 are obtained. The changes from the initial state are obvious, but one easily can also see that some short wavelength oscillations are still present. It should be noted that due to lateral averaging in a reflectivity scan the lateral resolution of X-ray reflectometry is of the order of several micrometers.[18] The Voronoi pattern of droplets dispersed on the substrate thus is for X-ray reflectometry equivalent to a very rough polymer film of reduced density. However, the reflectivity curves obtained from dewetted samples cannot be fitted to a single rough polymer layer. Moreover, Figure 8 clearly shows that the low-frequency oscillations of the reflectivity curves depend on the molecular weight of the chains. The lowest frequency (corresponding to the thinnest films) is produced for the lowest molecular

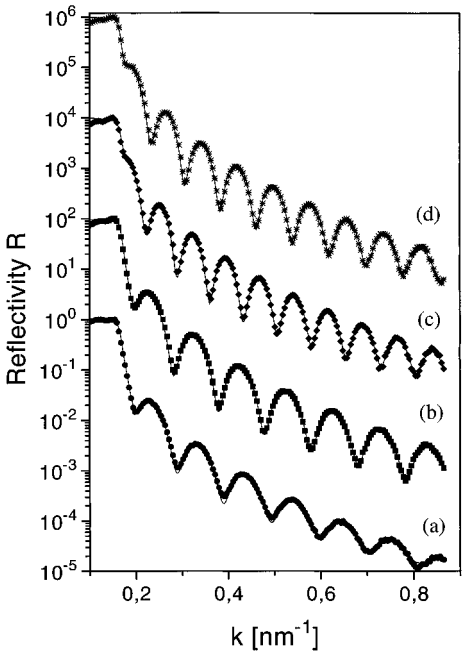

Figure 7. X-ray reflectivity curves versus z-component of incident wavevector, k, for thin films of ω-barium sulfonato polystyrene before annealing. Molecular weights of the materials were $\bar{M}_n = 2800$ (●), 13 000 (■), 18 000 (◆), and 19 500 (*). Reflectivities of different samples are multiplied with a factor of 10^2 (■), 10^4 (◆), and 10^6 (*). The film thicknesses are 39 (*), 42 (◆), 31 (■), and 30 (●) nm, respectively. Solid lines are best fits to a single-layer model (see text).

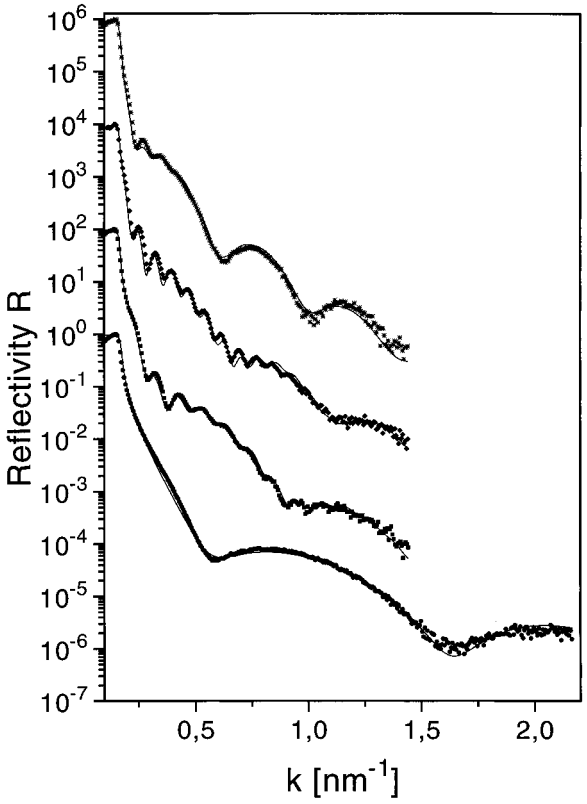

Figure 8. X-ray reflectivity curves versus incident wavevector, k, for thin films of ω-barium sulfonato polystyrene after annealing for 200 h at 175 °C. Symbols and scaling are the same as in Figure 7, while the k-axis has been expanded. Solid lines are best fits to a two-layer model described in the text.

weight ($\bar{M}_n = 2800$). This observation suggests that a monolayer of adsorbed polymer remains adsorbed at the surface of the silicon wafer, even after annealing for 200

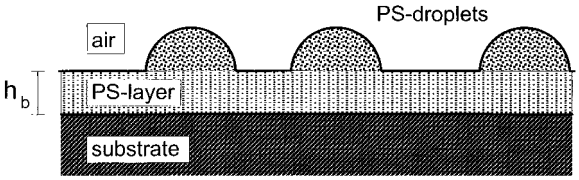

Figure 9. Schematic illustration of a cross section through a dewetted film. A thin uniform film of thickness h_b is remaining on the substrate. On top of the film small droplets of dewetted polystyrene are formed.

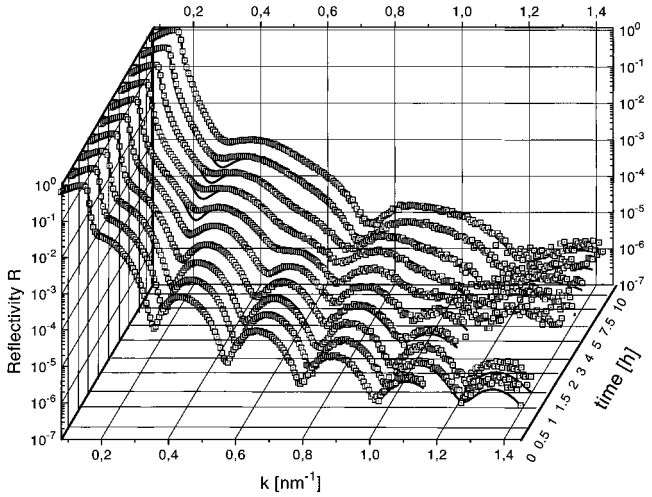

Figure 10. Typical evolution of the X-ray reflectivity curves as a function of annealing time ($T = 175$ °C) for an ω-barium sulfonato polystyrene ($\bar{M}_n = 13\,000$, initial film thickness $h = 15$ nm). Solid lines are best fits based on density profiles shown in Figure 11.

h at 175 °C. Therefore, the fits to the experimental curves of Figure 8 have been generated using a model that assumes that a thin homogeneous bottom layer is surmounted by a thicker, very rough layer of reduced density (simulating the droplets of dewetted film). The situation is schematically shown in Figure 9.

The typical time dependence of the X-ray reflectivity curves is depicted in Figure 10. Major changes occur during the first 10 h of annealing time, while no significant changes can be detected for longer annealing times (up to 200 h). The high-frequency oscillations that characterize the initial homogeneous film are progressively damped and smeared out, while low-frequency oscillations emerge and become rather well defined at the end of the dewetting process.

Figure 11 shows the corresponding electron density profiles, obtained from the fits to the reflectivity curves for a film of initial thickness $h = 14$ nm. The progressive dewetting of the polymer film is evident, as well as the existence of a thin adsorbed polymer layer of a few nanometer thickness. Figure 11 also clearly shows that droplet formation is associated with a decrease in electron density, since X-ray reflectometry probes a laterally averaged electron density intermediate to that of polystyrene (in the droplets) and air (between the droplets). The thickness of the thin adsorbed layer is essentially independent of the initial film thickness as shown in Figure 12 for two different molecular weight samples. The layer thickness is constant for a given molecular weight but depends strongly on the molecular weight of the ω-barium sulfonato polystyrene. This behavior is in complete agreement with the assumption that the bottom layer consists of an adsorbed polymer brush of polystyrene chains tethered to the silicon oxide

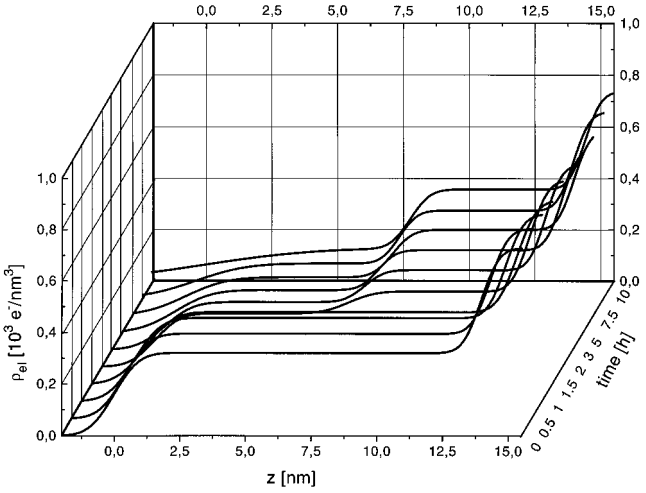

Figure 11. Evolution of the electron density profile perpendicular to the surface (in *z*-direction) as a function of annealing time (T = 175 °C) for the sample of Figure 10. The electron density profiles have been obtained from fits to the data of Figure 10.

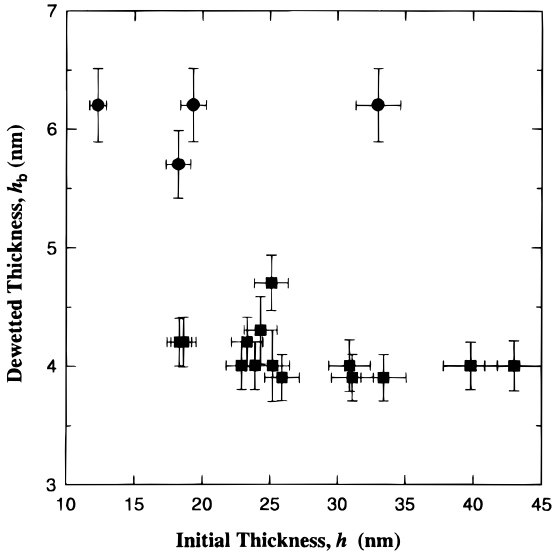

Figure 12. Monolayer film thickness after dewetting, h_b, as a function of initial film thickness, h, for ω-barium sulfonato polystyrene with $\bar{M}_n$ = 2800 (■) and 13 000 (●). Films were annealed for 200 h at 175 °C.

surface. Films of thickness equivalent to that of the adsorbed brush remain unaffected by annealing. No changes in the reflection curves are observed for a film of initial thickness h = 5 nm after 100 h of annealing at 175 °C as shown in Figure 13. Reflection curves can be fitted by a single layer model assuming a constant electron density within the film. Thus the interaction of the adsorbed brush with the substrate is very strong. The thickness of this uniform layer is expected to depend on the molecular weight of the chains only and to scale linearly with the radius of gyration of the chains. This behavior is observed as expected for slightly stretched chains and can be seen in Figure 14, where the average adsorbed layer thickness h_b is plotted against the diameter (2 times the radius of gyration) of the chains for four different molecular weights. Within the limits of the experimental errors, the thickness of the adsorbed layer depends linearly on the size of the chains.

From the fits to the experimental reflection data (Figure 8), one obtains the electron density ρ_{el} and also

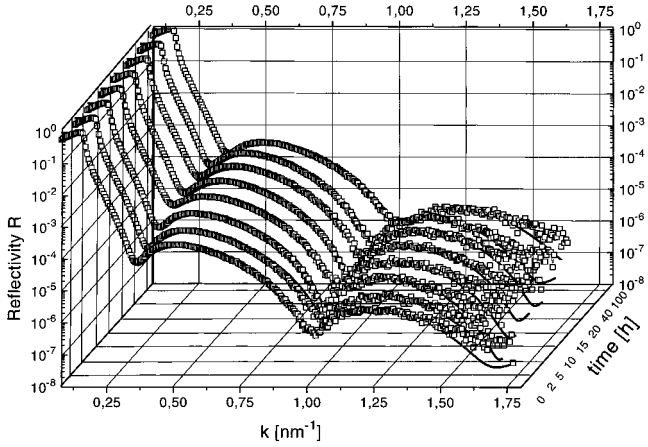

Figure 13. X-ray reflectivity curves as a function of annealing time (T = 175 °C) for an ω-barium sulfonato polystyrene ($\bar{M}_n$ = 13 000, initial film thickness h = 5 nm). Solid lines are best fits to the single-layer model described in the text.

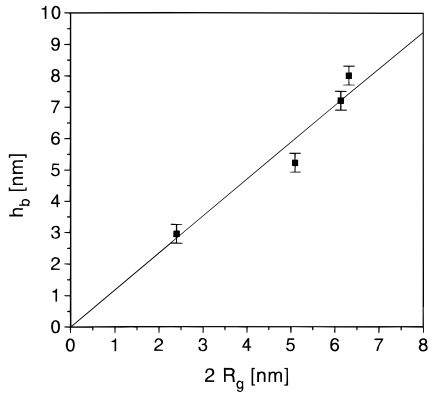

Figure 14. Monolayer film thickness after dewetting, h_b, versus radius of gyration of the polystyrene chains, R_g, for the different investigated monofunctional samples.

the density ρ of the adsorbed brush (Table 4). The amount of adsorbed polymer A can be calculated from eq 12:

$$A = \rho h_b \tag{12}$$

The grafting density, σ (nm^{-2}), *i.e.*, the inverse of the average area per adsorbed chain, can be determined by eq 13:

$$\sigma = \frac{A}{M_w} N_A 10^{-18} \,(\mathrm{nm}^{-2}) \tag{13}$$

where N_A is Avogadro's number.

Accordingly the mean interchain spacing between adsorbed chains, D_{inter}, can be calculated from:

$$D_{inter} = \sigma^{-1/2} \tag{14}$$

The experimental value of D_{inter} will be compared with the interchain spacing of unperturbed chains D_{over}, which is estimated using the following equations:

$$D_{over} = \sqrt{\pi} R_{PS} \tag{15}$$

$$R_{PS} = 1.86 N_S^{0.595} \tag{16}$$

R_{PS} is the Flory radius of polystyrene in toluene solution, N_S is the mean degree of polymerization, and D_{over}

Table 4. Experimentally Determined Parameters (As explained in the text) of Different Monofunctional Polystyrenes of Low Molecular Weight

M_n (g/mol)	N_S	ρ_{el} (10^3 e$^-$/nm^3)	ρ (g/cm^3)	h_b (nm)	A (mg/m^2)	σ (nm^{-2})	D_{inter} (nm)	R_{PS} (nm)	D_{over} (nm)	D_{inter}/D_{over}
2800	27	0.321	0.9899	3.0	2.97	0.60	1.30	1.32	2.34	0.55
13 000	122	0.328	1.0115	5.0	5.06	0.22	2.14	2.41	4.27	0.50
18 000	177	0.318	0.9807	7.2	7.06	0.22	2.11	3.24	5.74	0.37
19 500	187	0.321	0.9899	8.0	7.91	0.23	2.07	3.43	6.08	0.34

corresponds to the distance between two unperturbed polymer coils that come into contact. Thus the ratio D_{inter}/D_{over} gives a measure of the chain conformation in the brush. For polymer chains in their unperturbed conformation, the ratio equals 1. A ratio larger than 1 means uncomplete coverage of the surface or a conformation, where the chains are lying flat on the surface as compared to their unperturbed conformations. In the case of a ratio smaller than 1, the polymer chains can be expected to be in a stretched conformation. The determined values of the investigated samples are listed in Table 4. In all cases, the D_{inter}/D_{over} ratios are considerably smaller than 1 and decrease with increasing molecular weight. The ratios vary between 0.34 and 0.55, *i.e.*, the chains are stretched by factors between 2 and 3 compared to their unperturbed dimensions. Thus the chains may be markedly stretched but not in a true brushlike conformation of highly extended chains. It should be mentioned that those considerations can only be applied assuming that all chains in the layer have their functional ends tethered to the substrate and that significant interpenetration does not occur.

Similar conclusions have been drawn from adsorption experiments of ω-lithium and -barium sulfonato polystyrenes from toluene solutions.[16] Ellipsometric measurements reveal that the chains adsorbed on the silicon surface are densely packed and significantly stretched in the solution. The presence of a single sulfonate end group therefore significantly changes the adsorption and wetting behavior of polystyrene chains onto silicon oxide surfaces. Whereas unfunctionalized polystyrene completely dewets the silicon oxide surface when heated above T_g, the functionalized chains seem to form a brush of tethered chains that remain strongly adsorbed even at temperatures well above T_g (*e.g.*, at 175 °C). The ionic groups are completely buried below the polystyrene chains, since contact angle measurements on the adsorbed monolayers do not reveal any difference with the values reported for homopolystyrene films. The adsorption of the ω-barium sulfonato polystyrenes thus results in a complete coverage of the silicon surface, and the coated surface is expected to behave in most respects like a polystyrene surface.

Surprisingly enough, however, the observed dewetting behavior with thicker films clearly shows that the bottom polystyrene monolayer is markedly different from a normal polystyrene surface. If both tethered and nonadsorbed polystyrenes exhibit exactly the same properties, then the Hamaker constants for liquid−liquid (A_{ll}) and solid−liquid (A_{sl}) interactions would be exactly the same, and the effective Hamaker constant, A, would be zero. As a result, no disjoining pressure would exist in the film, and dewetting would not occur. In other words, polystyrene should wet polystyrene. The dewetting of the films reveals that the interactions between the unadsorbed polystyrene chains in the liquid state are more favorable than the interactions between these chains and the polymer brush. A similar behavior has been reported by Yerushalmi *et al.*,[14] who observed dewetting of low molecular weight polystyrene thin films at the surface of an adsorbed polystyrene brush. They used, however, a low molecular weight liquid, where only a small amount of higher molecular weight polymer is dissolved. The observed behavior may be explained by the particular conformation of the chains in the polymer brush, which might repel other macromolecules and prevent significant interpenetration with the adsorbed chains. The presence of the dense polymer brush might also explain the anomalous flow behavior observed during dewetting. The dewetting ω-barium sulfonato polystyrene, as previously mentioned, has been found to slip, in agreement with theoretical predictions. Slippage is a consequence of the nonwetting behavior of the liquid film on the surface. In the case of ω-barium sulfonato polystyrene, however, the liquid polystyrene dewets a polystyrene surface, due to the formation of a dense brush layer of functional chains. Slippage might occur due to the reduced interactions between the chains of the brush and those of the liquid layer.

The densely packed tethered chains can hardly accommodate other polymer chain segments, and penetration of unadsorbed chains into the brush is only partially possible. Thus for entropic reasons an existing difference in free energy between the dry brush and the molten chains results in an interfacial tension at the interface between chemically identical macromolecules, as recently also proposed by Leibler.[22] The spreading coefficient becomes negative, and a small non-zero equilibrium contact angle is expected. Therefore, dewetting between chemically identical chains becomes possible, and the molten chains slip on top of the brush according to theory. A similar behavior is also predicted from calculations of Binder *et al.*,[23] where a free chain is observed to be expelled from a dense layer of brushlike tethered chains.

High Molecular Weight ω-Barium Sulfonato Polystyrenes. High molecular weight ($\bar{M}_n$ = 82 000 and 98 000) ω-barium sulfonato polystyrene films do not show clear signs of dewetting after 6 weeks of annealing at 175 °C. Thus dewetting kinetics in high molecular weight samples are much slower than in low molecular weight samples due to an increase in viscosity with molecular weight. Rheology measurements show that viscosity changes from 500 P (M_n = 19 400 g/mol) to 35 000 P (M_n = 82 000 g/mol), *i.e.*, by a factor of 70. This means films of high molecular weight samples can kinetically stabilize by increasing molecular weight. This effect could be attributed to the presence of entanglements between the adsorbed polymer brush and the macromolecules in the film. For polystyrene, the critical molecular weight for entanglement, M_e, is of the order of 30 000.[20] Since the investigated low molecular weight ω-functional chains are well below M_e, no entanglements can prevent the films from dewetting. The high molecular weight samples, in contrast, are well beyond M_e, and entanglements between the brush and free long chain polymers therefore may play an essential role in the stability of the spin-coated polymer films.

α,ω-Barium Sulfonato Polystyrenes. Interestingly enough, no dewetting is observed when thin films of difunctional polystyrene chains are annealed, regard-

less of the molecular weight of the chains. The thickness of films prepared from low molecular weight samples ($\bar{M}_n = 8000$ and 14 000) decreases by about 10% after annealing for up to 200 h at 175 °C, but no further changes can be detected, and no holes are formed. No change at all can be detected for films prepared from the high molecular weight material ($\bar{M}_n = 102\ 000$). The observed thickness decrease could arise from a homogenization of stresses in the film during annealing, which would be less pronounced for the high molecular weight sample.

Obviously, the introduction of a second ionic group at the end of the chains deeply influences the wetting behavior of the low molecular weight materials. It is worth recalling that the metal sulfonate end groups have been shown to aggregate into small ionic domains containing about 12 ion pairs, both in bulk and in apolar solvents.[17] In the case of α,ω-ionic polymer chains, the ionic aggregates act as thermoreversible cross-links and are the reason for the improved rheological and mechanical properties of these materials.[17,21] These metal sulfonate ionic aggregates are thermally very stable up to temperatures of 300 °C.[21] Therefore, the presence of ionic aggregates might explain the stability of the thin films of α,ω-barium sulfonato polystyrene. The aggregates would act as cross-links in the material and would be responsible for the connection of the polymer film with the adsorbed polymer brush. At the moment one cannot decide whether this stabilization is a thermodynamic or kinetic effect. Viscosity of difunctional samples also varies with molecular weight. Viscosities increase from 84 000 P ($\bar{M}_n = 23\ 500$) to 450 000 P ($\bar{M}_n = 102\ 000$), *i.e.*, viscosities of difunctional samples are much higher than viscosities of monofunctional samples (see above). However, the molecular weight dependency of viscosity of difunctional samples is not as pronounced as for monofunctional samples. Stabilization of difunctional films might be a kinetic effect. On the other hand, stabilization of such films might also be thermodynamically controlled due to a cross-linking between different ionic aggregates as discussed below (see Figure 15). Investigations concerning this question are presently under way.

Figure 15 schematically illustrates the possible organization in thin films of both mono- and difunctional polystyrene chains. For monofunctional chains, only the unfunctionalized ends are present at the polystyrene side. Moreover, ionic group aggregation gives rise to starlike aggregates in the melt, which are not interconnected and may thus easily flow and rearrange at the surface of the brush. For difunctional samples, the situation is quite different. Provided that some of the difunctional chains are not adsorbed at the substrate via both ionic end groups, the dangling ionic ends may anchor the aggregates in the melt to the polymer brush. Since the ionic aggregates are interconnected by the difunctional chains, the polymer film is physically cross-linked and dewetting cannot take place. This interpretation is supported by recent ellipsometric measurements on the adsorption behavior of α,ω-barium sulfonato polystyrenes from solution, which are similarly in favor of a multilayer adsorption due to ionic aggregation.[16]

Conclusions

ω- And α,ω-barium sulfonato polystyrenes have been shown to interact strongly with clean silicon oxide surfaces, regardless of the molecular weight and functionality of the chains. Short monofunctional chains

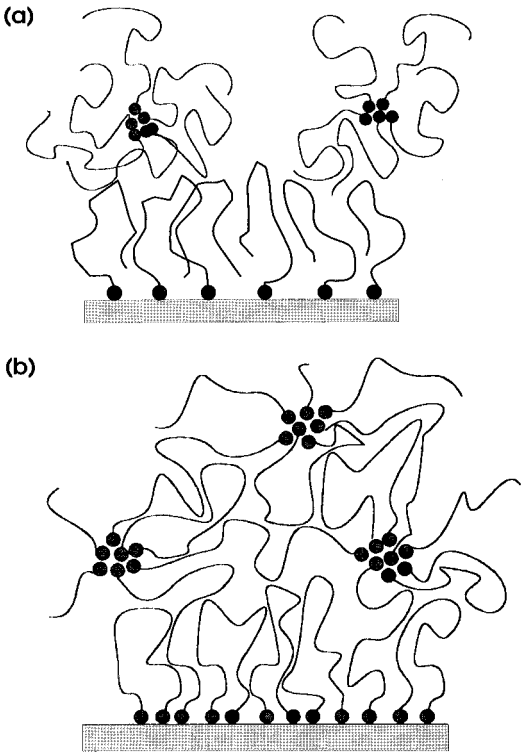

Figure 15. Schematic model of the films for (a) ω-metal sulfonato polystyrene and (b) α,ω-metal sulfonato polystyrene. Ionic end groups are marked by black dots.

form a densely packed polymer brush layer which completely coats the silicon surface. In the brush layer, the chains are significantly stretched and can hardly accommodate other polymer chain segments. As a result, upon annealing at temperatures higher than T_g of polystyrene, a liquid polymer film on top of the brush layer is unstable and spontaneously dewets the adsorbed layer. As a result of the dewetting process, a Voronoi cell pattern of hemispherical liquid polymer droplets is formed, whose parameters depend on the initial film thickness in the same way as in normal polystyrene films.[9] This process, however, takes place on an adsorbed brushy monolayer, and the polystyrene chains slip due to the presence of the adsorbed polystyrene brush leading to a nonlinear $^2/_3$ power law time dependence.

When the molecular weight of the monofunctional chains is large enough to allow the macromolecules to entangle, dewetting is retarded, and it is reasonable to assume that entanglements between the adsorbed and unadsorbed polymer chains are formed. Since these entanglements also occur with unfunctionalized polystyrene chains,[14] the addition of a small amount of ω-metal sulfonato polystyrene to normal polystyrene should be sufficient to retard the dewetting of thin polystyrene films. This effect, however, will only take place if a sufficient amount of the functionalized polymeric "additive" diffuses to the surface and acts as an anchor for the film. Additional measurements are in progress in order to determine more precisely the critical amount and critical molecular weight of functional chains required to retard dewetting.

The adsorption of difunctional chains is analogous to that of the monofunctional counterparts. However, ionic group aggregation is responsible for physical cross-links in the material. No dewetting occurs, even for the lowest molecular weights investigated. Thus part of the adsorbed difunctional chains may not be adsorbed by

both ends, and dangling ionic ends are expected to link the unadsorbed difunctional chains to the polymer brush via ionic aggregation. This effect is similar to that of chain entanglements but cannot take place with unfunctionalized polystyrene.

The introduction of functionalities in ω- and α,ω-metal sulfonato high molecular weight polymer chains has been shown to improve the thermal stability of thin polymer films. These properties should deserve more interest in the near future, since numerous technological applications, like thin dielectric films, nonlinear optics, and coatings, might benefit from an increased working temperature range and thin film stability.

Acknowledgment. The authors would like to thank M. Bach for technical help during the X-ray experiments. Helpful discussions with Prof. J. P. Rabe, Dr. M. Rücker, Prof. Binder, and Prof. Leibler are gratefully acknowledged. P.V. and R.J. are grateful to the Services Fédéraux des Affaires Scientifiques, Techniques et Culturelles in the frame of the Poles d'Attraction Interuniversitaires: Polymères for financial support, and P.V. also thanks the Belgian Fonds national de la Recherche Scientifique for a research fellowship. Financial support of G.H. by the BMFT (Grant 03-FI3MPG) is gratefully acknowledged.

References and Notes

(1) de Gennes, P.-G. *Rev. Mod. Phys.* **1985**, *57*, 827.
(2) Brochard, F.; Redon, C.; Rondelez, F. *C. R. Acad. Sci., Ser. 2* **1988**, *306*, 1143.
(3) Israelachvili, J. N. *Intermolecular and Surface Forces*; Academic Press: London, 1985.
(4) Srolowitz, D. J.; Safran, S. A. *J. Appl. Phys.* **1986**, *60*, 247.
(5) Sekimoto, K.; Oguma, R.; Kawasaki, K. *Ann. Phys. (N.Y.)* **1987**, *176*, 359.
(6) Brochard, F.; Daillant, J. *Can. J. Phys.* **1990**, *68*, 1084.
(7) Brochard-Wyart, F.; Redon, C.; Sykes, C. *C. R. Acad. Sci., Ser. 2* **1992**, *314*, 19.
(8) Brochard-Wyart, F.; de Gennes, P.-G.; Hervert, H.; Redon, C. *Langmuir* **1994**, *10*, 1566.
(9) Reiter, G. *Langmuir* **1993**, *9*, 1344.
(10) Redon, C.; Brzoska, J. B.; Brochard-Wyart, F. *Macromolecules* **1994**, *27*, 468.
(11) Redon, C.; Brochard-Wyart, F.; Rondelez, F. *Phys. Rev. Lett.* **1991**, *66*, 715.
(12) Silberzan, P.; Léger, L. *Macromolecules* **1992**, *25*, 1267.
(13) Halperin, A.; Tirrell, M.; Lodge, T. P. *Adv. Polym. Sci.* **1992**, *100*, 31.
(14) Yerushalmi-Rozen, R.; Klein, J.; Fetters, L. J. *Science* **1994**, *263*, 793.
(15) Parsonage, E.; Tirrell, M.; Watanabe, H.; Nuzzo, R. G. *Macromolecules* **1991**, *24*, 1987.
(16) Pankewitsch, T.; Stamm, M.; Vanhoorne, P.; Jérôme, R. *Macromolecules*, submitted.
(17) Vanhoorne, P.; Van den Bossche, G.; Fontaine, F.; Sobry, R.; Jérôme, R.; Stamm, M. *Macromolecules* **1994**, *27*, 838.
(18) Stamm, M. In *Physics of Polymer Surfaces and Interfaces*; Sanchez, I. C., Ed.; Butterworth-Heinemann: Boston, 1992.
(19) Foster, M.; Stamm, M.; Reiter, G.; Hüttenbach, S. *Vacuum* **1990**, *41*, 1441.
(20) Graessley, W. W. *Physical properties of polymers*; American Chemical Society: New York, 1984; Chapter III.
(21) *Structure and Properties of Ionomers*; Pinéri, M., Eisenberg, A., Eds.; NATO ASI Series C; D. Reidel: Boston, 1987; Vol. 198.
(22) Leibler, L.; Adjari, A. In *Ordering in Macromolecular Systems*; Teramoto, A., Kobayashi, M., Norisuje, T., Eds.; Springer-Verlag: Berlin, Heidelberg, 1994.
(23) Binder, K.; Lai, P. Y.; Wittmer, J. *Faraday Discuss.* **1994**, *98*, 97.

MA9500392